

Figure Sup1. All atom RMSD vs. time plot from MD simulations of the hexamer of Fig. 1 on the surface of a lipid bilayer.

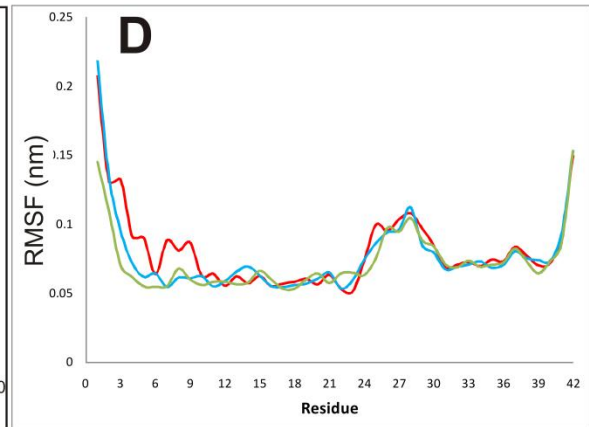
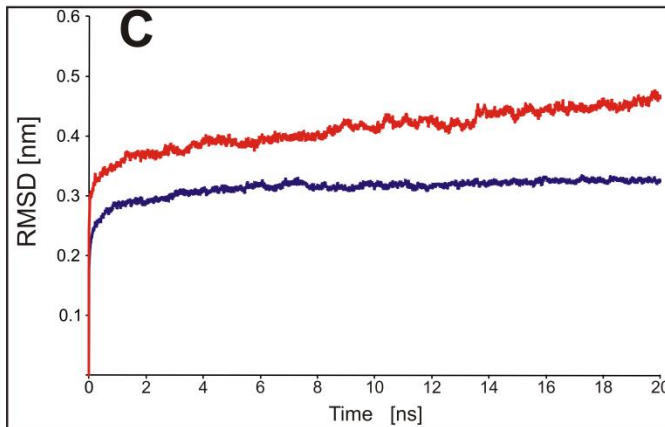
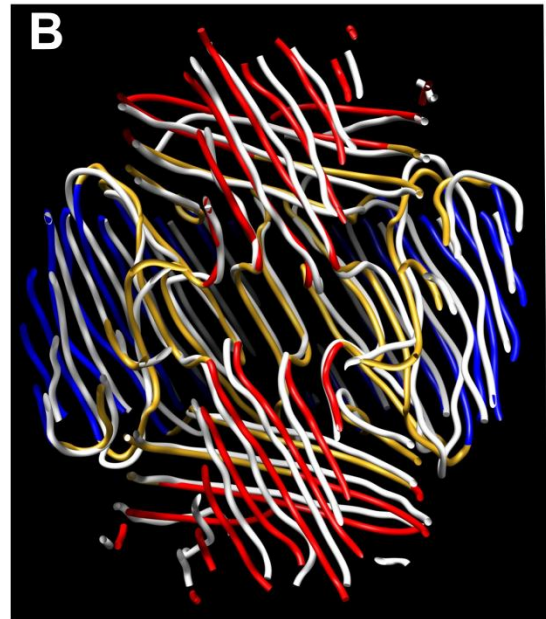
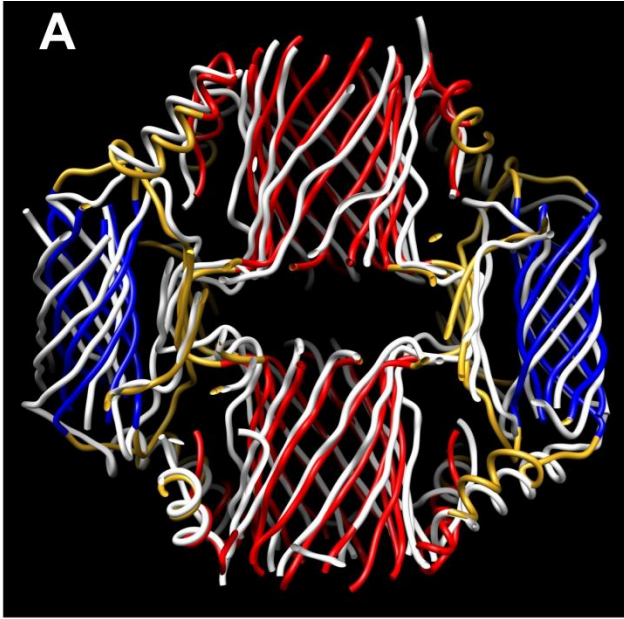


Figure Sup2. Results of MD simulations of (A) the hexamer-of-hexamer model of Fig. 3D and (B) the merged 36-mer of Fig. 3E. Backbone representations of the symmetrical models at the beginning of the simulation are colored by segment as in the text, and the averaged structures from the final 3 ns of 20ns simulations are white. (C) All atom RMSD vs. time plots for the model of (A) is red and that for the model of (B) is blue. (D) RMSF vs. residue numbers for the three subunit types (Sub<sub>1</sub> is blue, Sub<sub>2</sub> is green, and Sub<sub>3</sub> is red) of the final model of (B).

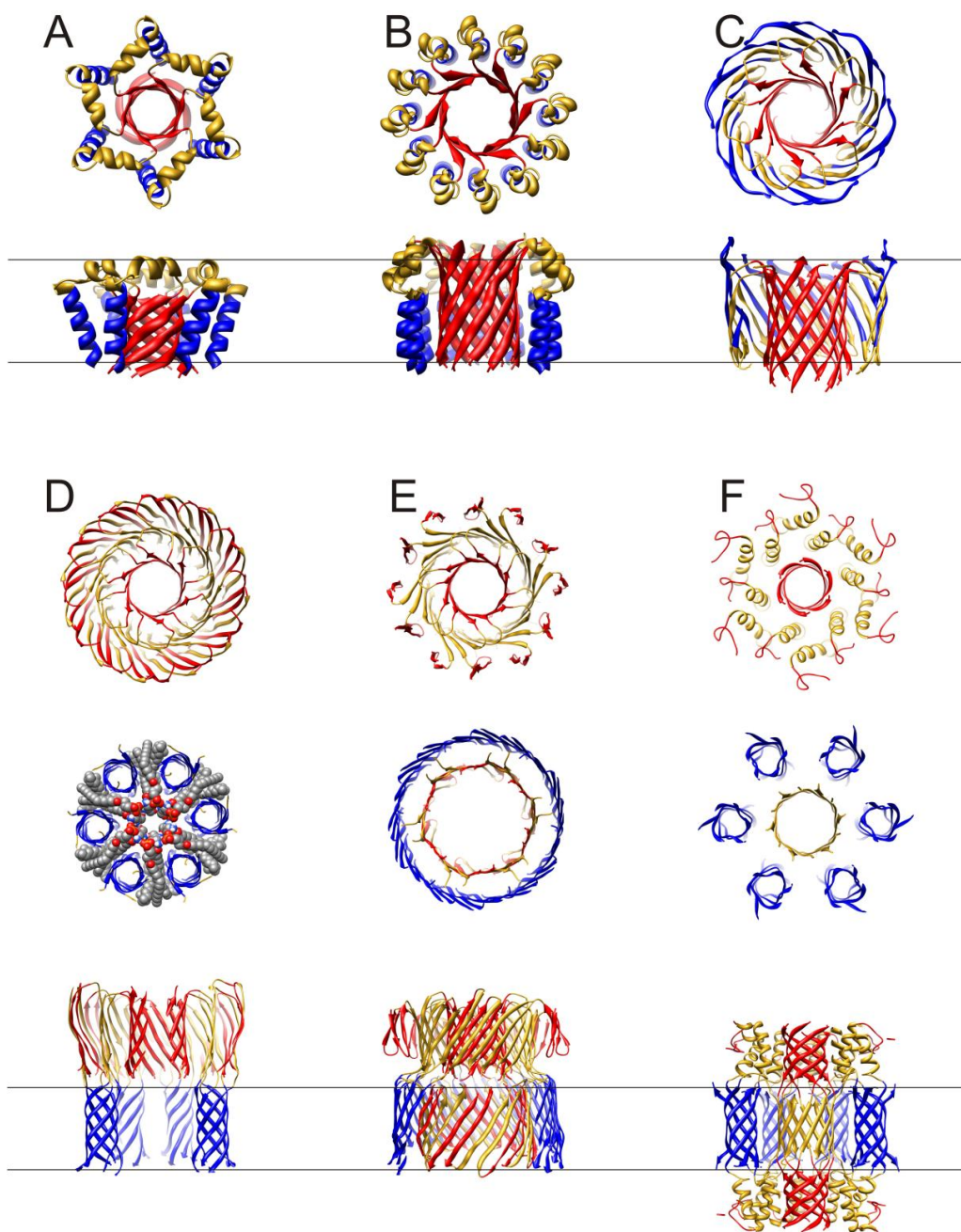


Figure Sup3. Ribbon representations of some alternative models not presented in the text. The structural description of these models are given in Supplement Table I. Segments are colored as in the text: S1-red, S2-gold, and S3-blue. For all models, the top row shows views from the trans side of the membrane through the central pore, and the bottom row shows side views with lines approximating the boundaries of the membrane's alkyl phase. Some segments have been clipped off in the side view to better illustrate structures of the core region. For D-F the top view has been separated into the aqueous-phase S1 and S2 segments (top row) and the transmembrane segments (middle row). The spaced-filled molecules colored by element type in the middle row of D are lipids postulated to line the pore.

Model	S1	S2	S3	Diameter (nm)	H-bonds/mon	RMSD (nm)
A, hexamer	6s-par- $\beta$ b	6 $\alpha$ -helix	6 $\alpha$ -helix	5.5	28.5	0.37
B, dodecamer	12s-par- $\beta$ b	12 $\alpha$ -helix	12 $\alpha$ -helix	5.4	32.1	0.39
C, dodecamer	12s-par- $\beta$ b	24s-ap-S2-S3- $\beta$ b	24s-ap-S2-S3- $\beta$ b	5.7	32.1	0.44
D, 36mer	12s-par- $\beta$ b 36s-S1S2- $\beta$ b	24s-par- $\beta$ b 36s-S1S2- $\beta$ b	6x6s-par- $\beta$ b	7.0	31.5	0.51
E, 36mer	12s-par- $\beta$ b $\beta$ -hairpin 24s-ap-S1S2 $\beta$ b	24s-par- $\beta$ b 24s-ap-S1S2 $\beta$ b	36s-par- $\beta$ b	7.7	35.9	0.37
F, 36mer	2x6s-par- $\beta$ b Random coil	24 $\alpha$ -helix 12s-ap- $\beta$ b	6x6s-ap- $\beta$ b	7.3	30.2	0.51
Fig. 3D 36mer	2x12s-par- $\beta$ b 12xS1-S1 $\beta$ -strand	24s-ap- $\beta$ b 12xS1-S2 $\beta$ -strand	6x6s-ap- $\beta$ b	8.5	31.6	0.45
Fig. 3E 36mer	2x12s-par- $\beta$ b 12xS1-S2 $\beta$ -strand	24s-ap- $\beta$ b 12xS1-S2 $\beta$ -strand	36s-ap- $\beta$ b	7.3	37.9	0.33

Supplement Table I. Properties of the models illustrated in Supplement Fig. Sup3 and Fig. 3 of the text. The structural motif or motifs of each segment is listed under the segment name, S1, S2, or S3. The nomenclature begins with the number of times the motif occurs in the assembly, #x, unless it occurs only once, then the number of stands (#s), then whether the motif is a parallel (par) or antiparallel (ap)  $\beta$ -barrel ( $\beta$ b). When more than one type of segment comprises the barrel, the segment names (S1S2 or S2S3) precede  $\beta$ b. The next column is the estimated maximum outer diameter of the assembly. H-bonds/mon indicates the number of non-aqueous H-bonds per monomer formed by the structure averaged during the last 3 ns of a 20 nm MD simulation. RMSD is the all atom root-mean-squared deviation from the initial symmetric model toward the end of the MD simulation. Note, RMSD tends to increase with the number of monomers, so apparently comparable values for the hexamer and dodecamers relative to the 36mers are somewhat misleading.

All of the models illustrated in Figure Sup3 have either six- or twelve-stranded parallel S1  $\beta$ -barrels with axes corresponding to the symmetry axis of the pore. Thus, these models are all consistent with the hypothesis that parallel S1 $\beta$ -barrels form part of the permeation pathway, and that putative channel blockers act by binding to the E11-H14 portion of these barrels. Predominately helical models (A & B) are not considered likely because: membrane-bound A $\beta$  assemblies with > 3 subunits tend to have a predominantly  $\beta$  secondary structure<sup>2</sup>, the diameters of the assemblies are less than seen in the freeze fracture images of Fig. 1, and the number of non-aqueous H-bonds per monomer are lower than most of the other alternative models. The last two criticisms also apply to the dodecamer model C, which also has a relatively high RMSD (see

Supplement Table I). The primary advantage of model D (and similar antiparallel models not shown) is that there are no polar side chain atoms in the transmembrane region, and for the parallel model D no polar segments would need to enter or cross the transmembrane region during the insertion process. However, the major disadvantages are that these models are less stable (higher RMSDs), cannot explain data with Y10W mutants in which the mutated tryptophan appears to insert into the membrane<sup>2</sup>, and require greater perturbation of membrane lipids. Model E is similar to the final model of Fig. 3E in the main text, in that S3 segments form a 36-stranded  $\beta$ -barrel; however, the barrel is parallel in this case. On the positive, model E has higher H-bonding and lower RMSD values than all other models except for the final antiparallel model of Fig. 3E. It also has the advantage that it is more consistent with findings that at least some A $\beta$  channels appear to have asymmetric transmembrane orientations relative to putative channel blockers<sup>1</sup>. However, Model E forms fewer H-bonds and has higher RMSD values than its antiparallel analog (final model of Fig. 3E). Other models with a 36-stranded parallel S3 barrel can be envisioned; e.g., the S3 barrel could surround a parallel 24-stranded S2  $\beta$ -barrel, which in turn surrounds a parallel 12-stranded S1-barrel while the additional S1 and S2 segments extend into the aqueous phases. Similarly, the H-bonding and RMSD value of Model F are comparable to most other models with six 6-stranded S3  $\beta$ -barrels, and has the potential advantage that no polar S1 segments reside in the TM region. However, Model F and antiparallel models in which 6-stranded S3  $\beta$ -barrels are the only segments that reside in the TM region were not included in the text as part of the putative transition series because it is difficult to transition from these structures to the final model of Fig. 3E with the 36-stranded antiparallel S3  $\beta$ -barrel, which is more stable and has more H-bonds.

#### Reference List

1. Arispe N, Diaz JC, Simakova O. Abeta ion channels. Prospects for treating Alzheimer's disease with Abeta channel blockers. *Biochim Biophys Acta* 2007;1768:1952-1965.
2. Wong PT, Schauerte JA, Wisser KC, Ding H, Lee EL, Steel DG, Gafni A. Amyloid-beta membrane binding and permeabilization are distinct processes influenced separately by membrane charge and fluidity. *J Mol Biol* 2009;386:81-96.